JOURNAL OF AGRICULTURAL AND FOOD CHEMISTRY

Effect of Adlay (*Coix lachryma-jobi* L. var. *ma-yuen* Stapf) Testa and Its Phenolic Components on Cu^{2+}-Treated Low-Density Lipoprotein (LDL) Oxidation and Lipopolysaccharide (LPS)-Induced Inflammation in RAW 264.7 Macrophages

DIN-WEN HUANG,[†] YUEH-HSIUNG KUO,*[,‡,§] FANG-YI LIN,[†] YUN-LIAN LIN,*[,||] AND WENCHANG CHIANG*[,†]

Graduate Institute of Food Science and Technology, Center for Food and Biomolecules, College of Bioresources and Agriculture, National Taiwan University, Taipei 106, Taiwan, Tsuzuki Institute for Traditional Medicine, College of Pharmacy, China Medical University, Taichung 404, Taiwan, Agricultural Biotechnology Research, Academia Sinica, Taipei 115, Taiwan, and National Research Institute of Chinese Medicine, Taipei 112, Taiwan, Republic of China

The aims of this study were to investigate the effects of adlay testa (AT) on Cu^{2+}-treated low-density lipoprotein (LDL) oxidation, 2,2′-diphenyl-1-picrylhydrazyl (DPPH)-scavenging capacity, and lipopolysaccharide (LPS)-induced inflammation in RAW 264.7 macrophages and determine its active components. The AT ethanolic extract (ATE) was partitioned into four fractions by various solvents as follows: *n*-hexane (ATE-Hex), ethyl acetate (ATE-Ea), *n*-butanol (ATE-Bu), and water (ATE-H_2O). ATE-Ea and ATE-Bu were further fractionated into ATE-Ea-a−ATE-Ea-h and ATE-Bu-A−ATE-Bu-F, respectively, by column chromatography. Results showed that ATE-Ea, ATE-Bu, ATE-Ea-e, and ATE-Bu-C expressed antiradical, antioxidative, and anti-inflammatory activities with respect to the DPPH-scavenging capacity, LDL protection effect, and nitric oxide (NO) inhibitory activity. Inflammation was further modulated by ATE-Ea, ATE-Bu, ATE-Ea-e, and ATE-Bu-C through downregulating the expression of inducible nitric oxide synthase (iNOS) and cyclooxygenase 2 (COX-2) proteins. The following components were found in ATE-Ea-e and ATE-Bu-C after purification and high-performance liquid chromatographic analysis: chlorogenic acid (CGA), vanillic acid (VA), caffeic acid (CA), *p*-coumaric acid (PCA), ferulic acid (FA), and 2-*O*-β-glucopyranosyl-7-methoxy-4(^{2}*H*)-benzoxazin-3-one (GMBO). Results showed that CGA, CA, and FA were the major components responsible for the antioxidative and anti-inflammatory activities of ATE-Ea-e and ATE-Bu-C. Subsequently, each gram of ATE-Bu-C had 30.3 mg of CGA, 9.02 mg of CA, and 189 mg of GMBO, while each gram of ATE-Ea-e had 1.31 mg of VA, 3.89 mg of PCA, and 47.6 μg of FA. In conclusion, ATE has antioxidative and anti-inflammatory activities, and its effects are partially related to its phenolic components. Thus, ATE has the potential to be developed as a functional food targeting chronic diseases.

KEYWORDS: Adlay; antioxidative; anti-inflammatory; LDL; DPPH; NO; iNOS; COX-2

INTRODUCTION

Atherosclerosis is a chronic and complicated disease, leading to significant mortality in both the Western world and developing countries. Many recent studies have noted that the increasing formation of reactive oxidative species (ROS) and inflammation play important roles in atherosclerosis. An increase in the low-density lipoprotein (LDL) content causes the early phase of atherosclerosis, according to the oxidative modification hypothesis; oxidation of LDL is the most likely cause of atherogenesis. The oxidation of LDL may be induced by various enzymes, free radicals, or other non-enzymatic mechanisms (*1*−*3*). Subsequently, oxidized lipids derived from LDL activate the nuclear factor (NF)-κB transcription factor, which was first identified by Sen and Baltimore (*4*), and this leads to the induction of the expression of many early genes, such as inducible nitric oxide synthase (iNOS) and cyclooxygenase 2

* To whom correspondence should be addressed. Telephone: 886-2-33661671. E-mail: yhkuo@ntu.edu.tw (Y.-H.K.); Telephone: 886-2-28201999-6531. E-mail: yllin@nricm.edu.tw (Y.-L.L.); Telephone: 886-2-33664115. E-mail: chiang@ntu.edu.tw (W.C.).

[†] National Taiwan University.

[‡] China Medical University.

[§] Academia Sinica.

[||] National Research Institute of Chinese Medicine.

10.1021/jf803255p CCC: $40.75
Published on Web 02/25/2009

(COX-2). Nitric oxide (NO) and prostaglandin E (PGE), which can be produced either by NOS or COX-2, have been implicated in a variety of pathophysiological conditions, especially in the processes of atherosclerosis (*1*, *4*).

Adlay (*Coix lachryma-jobi* L. var. *ma-yuen* Stapf) or Job's tears is an annual crop that has been consumed as both a herbal medicine as a diuretic, anti-inflammatory, antitumor, and analgesic agent and a food supplement in traditional Chinese medicine (*5*). Air-dried adlay seeds are separated into four parts from the inside out, including the adlay hull (AH), adlay testa, adlay bran, and polished adlay. When the hull is removed, a thin fibrous layer called the pericarp can be seen. Immediately under the pericarp layer is the testa, which is only a few cells thick, but is less fibrous than the pericarp layer. Sometimes this layer is considered a part of the seed coat, but it is normally considered the outermost layer of the bran (*6*). Recent studies indicated that different parts of adlay may possess various physiological activities as follows: (1) antioxidative activity, the butanolic fraction of the the methanolic extract of the adlay hull (AHM-Bu) expressed strong antioxidative activity, and six components were purified from the adlay hull, including phenolic components and lignan (*7*); (2) anti-inflammatory activity, the methanolic extract of the adlay seed (ASM) inhibited NO formation in RAW 264.7 macrophage cells treated with LPS and interferon-γ (*8*); (3) endocrine modulation, both the ethyl acetate fraction of AHM and the butanolic fraction of the methanolic extract of adlay bran decreased progesterone and estradiol via different pathways (*5*, *9*); and (4) antitumor, the chemopreventive effect of ASM was also investigated *in vivo* by the tobacco-specific carcinogen, 4-(methylnitrosamino)-1-(3-pyridyl)-1-butanone (NNK), in A/J mice, and the number of surface lung tumors was reduced by ~50% (*10*). Dehulled adlay also suppressed an early event in colon carcinogenesis through downregulating the expression of COX-2 protein in azoxymethane (AOM)-induced carcinogenesis in F344 rats (*11*), and five active compounds that inhibited cancer cells were isolated from the adlay bran (*12*).

As discussed above, the various parts of the adlay seed have numerous physiological activities; however, the antiatherogenic effects of adlay testa (AT) are still unknown. Thus, prevention of oxidation of LDL, inflammatory response of the LPS-induced inflammatory system, and the active components were investigated in this study.

MATERIALS AND METHODS

Materials. 2,2′-Diphenyl-1-picrylhydrazyl (DPPH), 2-thiobarbituric acid (TBA), 6-hydroxy-2,5,7,8-tetramethylchroman-2-carboxylic acid (Trolox), and lipopolysaccharide (LPS) were obtained from Sigma Chemical (St. Louis, MO). Copper(II) sulfate pentahydrate ($CuSO_4 \cdot 5H_2O$) for LDL oxidation was obtained from Nacalai Tesque (Kyoto, Japan). Anti-iNOS and anti-COX-2 antibodies were purchased from Upstate (Lake Placid, NY) and BD Biosciences (San Jose, CA), respectively. The anti-β-actin antibody was obtained from Santa Cruz Biotechnology (Santa Cruz, CA). The compatible horseradish peroxidase (HRP)-conjugated secondary antibodies, goat anti-rabbit immunoglobulin G (IgG) and goat anti-mouse antibodies, were purchased from Pierce (Rockford, IL) and CHEMICON International (Temecula, CA), respectively.

Preparation of the Ethanolic Extracts and Various Fractions from the Testa of Adlay Seeds. The AT was obtained according to the procedure described by Hsia et al. (*5*). AT (12 kg) was extracted 3 consecutive times with ethanol (95%, 120 L) at room temperature for 24 h and filtered. The filtrate was concentrated under a vacuum to dryness, affording 538 g (4.48%, based on the dry weight) of an ethanolic extract, which was then stored at −20 °C. The ethanolic extracts of AT are referred to as ATE. ATE was then suspended in water with 10% methanol and partitioned with hexane until the hexane fraction was colorless. Thereafter, the hexane fraction (144 g, 1.2%, ATE-Hex) was obtained and dried under a vacuum. The defatted ATE was then partitioned with ethyl acetate (EA) to prepare the EA fraction (160 g, 1.33%, ATE-Ea). The residue was then partitioned with butanol and dried as described above to obtain the butanolic fraction (50 g, 0.42%, ATE-Bu). The aliquot fraction was freeze-dried to form the H_2O fraction (122 g, 1.02%, ATE-H_2O). The antioxidative (Cu^{2+}/LDL system), antiradical (DPPH radical system), and anti-inflammatory (LPS/RAW 264.7 cells system) activities of the various fractions were examined. ATE-Ea was subjected to column chromatography on silica gel and eluted using a hexane/EA/MeOH gradient with monitoring at 280 and 340 nm to afford eight subfractions: a (~0−10% EA/Hex), b (~10−20% EA/Hex), c (~20−30% EA/hex), d (~30−50% EA/Hex), e (~50−80% EA/Hex), f (~80−100% EA/Hex), g (~0−20% MeOH/EA), and h (~20−100% MeOH/EA). Each fraction was manually collected and concentrated at 60 °C under a vacuum. The ATE-Bu fraction was subjected to column chromatography with Diaion HP-20 resin, eluted by a H_2O/MeOH gradient to afford subfractions A (100% H_2O/MeOH), B (90% H_2O/MeOH), C (75% H_2O/MeOH), D (50% H_2O/MeOH), E (25% H_2O/MeOH), and F (0% H_2O/MeOH). Each fraction was manually collected and concentrated as described above. The activities of various subfractions were tested in the systems described above, and the bioguided subfractions ATE-Ea-D−ATE-Ea-F were combined and further purified by column chromatography (silica gel, eluted with 50−80% EA/Hex) and semi-preparative HPLC on a Lichrosorb si-60 column at 2 mL/min, using 30−50% EA/Hex as the eluent to yield vanillic acid (VA), 4-hydroxyacetophenone (4HA), syringaldehyde, and 6-methoxy-3*H*-benzoxazol. ATE-Bu-C−ATE-Bu-F were also combined and further purified by column chromatography (Sephadex LH-20 resin, eluted with MeOH; RP-18, eluted with 30% H_2O/MeOH) to yield chlorogenic acid (CGA), caffeic acid (CA), and 2-*O*-β-glucopyranosyl-7-methoxy-4(^2H)-benzoxazin-3-one (GMBO). The structures of all purified compounds were further identified by nuclear magnetic resonance (NMR, Bruker AMX-400) and compared to an authentic sample. **Figure 1** shows the schematic for the preparation of antioxidation and anti-inflammatory fractions from AT.

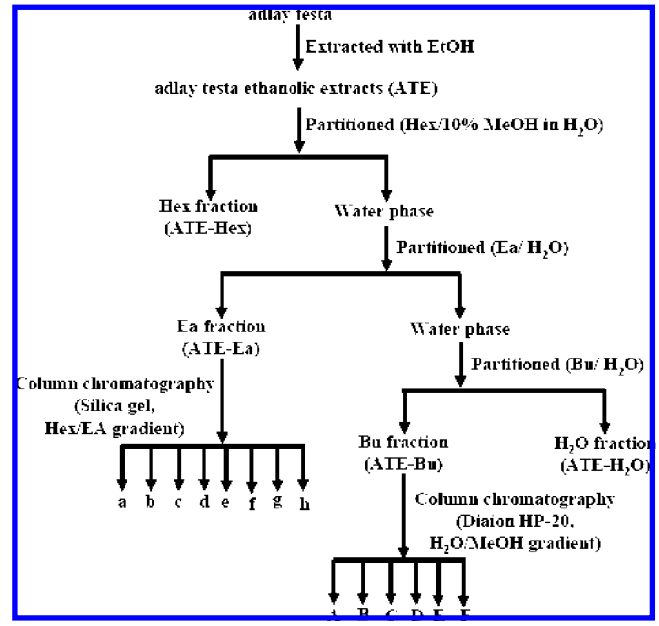

Figure 1. Scheme for extracting, partitioning, and fractionating of antioxidative and anti-inflammatory fractions from AT. ATE-Ea, ATE-Bu, ATE-Ea-e, and ATE-Bu-C exhibited the most potent inhibitory activities against oxidative stress and inflammation.

High-Performance Liquid Chromatographic (HPLC) Analysis. The analyses were performed according to Yen et al. (*13*), and carried out with a Hitachi L-6200 intelligent pump equipped with a photodiode array detector (Hitachi L-7455) and an automatic injector. A C18 (150 × 4.6 mm, 5 μM) reverse-phase column was used. Gradient elution

was performed with water−2% acetic acid (v/v, solvent A) and water−0.5% acetic acid/acetonitrile (1:1, v/v, solvent B) at a constant flow rate of 1 mL/min. Initial starting conditions were 5% B, 0−10 min B increased from 5 to 10%, 10−40 min B increased from 10 to 40%, 40−55 min B increased from 40 to 55%, 55−60 min B increased from 55 to 80%, 60−65 min B increased from 80 to 100%, 65−70 min B decreased from 100 to 50%, 70−75 min B decreased from 50 to 30%, 75−80 min B decreased from 30 to 10%, and 80−85 min B decreased from 10 to 5% and then switched to the original starting conditions (5% B).

LDL Preparation. Whole blood from healthy adult volunteers was collected in vacutainers containing ethylenediaminetetraacetic acid (EDTA) (1 mg/mL) and centrifuged at 3000 rpm (Hettich, Mikro 22 R, Ramsey, MN) for 10 min to isolate the plasma. LDL was isolated from the plasma by density-gradient ultracentrifugation ($d = 1.024-1.050$) in a Beckmann model LE-80K ultracentrifuge using a 70 Ti rotor (Palo Alto, CA). The LDL layer was removed and dialyzed twice against 5 L of phosphate-buffered saline (PBS, pH 7.4), for 12−18 h. After dialysis, the protein concentration in the pooled LDL was determined using a Bio-Rad protein assay solution as described by the manufacturer. The LDL fraction was either used immediately or purged with nitrogen and stored at 4 °C.

Formation of Conjugated Diene (CD). CD formation was monitored by the method described by Bourne and Rice-Evans (*14*). To assess the ability of extracts to inhibit copper-mediated LDL oxidation, levels of CD were continually monitored (at 5 min intervals) at 37 °C by obtaining the ultraviolet (UV) absorbance at 232 nm. The dialyzed LDL was diluted with PBS to achieve a concentration of 150 μg of protein/mL, and 10 μL of the test sample was then added. Oxidation was initiated by the addition of a freshly prepared $CuSO_4$ solution (the final concentration was 10 μM), and the final volume of the preparation was adjusted to 250 μL by adding PBS. The formation of CD was continuously monitored by a multidetection microplate reader (Synergy HT, BIO-TEK, Atlanta, GA). The lag phase of LDL oxidation, defined as the time interval (min) between the intercept of the slope of the curve with the initial absorbance axis, was measured.

Thiobarbituric-Acid-Reactive Substances (TBARS). TBARS was monitored by the method described by Yagi (*15*). LDL (150 μg of protein/mL) was incubated at 37 °C in a water bath with Cu^{2+} (10 μM) in the presence or absence of the test sample for 12 h. In brief, 0.5 mL of a 25% (w/v) trichloroacetic acid (TCA) solution was added to the incubated LDL solution and centrifuged at 9830*g* for 20 min to denature and precipitate the protein, and then 0.5 mL of 1% TBA (dissolved in 0.3% NaOH) was added to the 0.5 mL suspension described above. The mixture was thoroughly shaken and heated in a water bath at 90−95 °C for 45 min. After the mixture had cooled to room temperature, 1.0 mL each of distilled water and butyl alcohol was added and the sample was shaken for 1 min. After centrifugation at 880*g* for 10 min, the butyl alcohol phase containing the TBARS was separated and its fluorescence value was measured at the respective excitation and emission wavelengths of 532 and 600 nm. The inhibitory activities were calculated as a percentage using the following formula:

$$\text{inhibitory activity (\%)} = \{1 - [(\text{fluorescence}_{\text{sample}} - \text{fluorescence}_{\text{control}})/(\text{fluorescence}_{\text{CuSO}_4\text{-treated}} - \text{fluorescence}_{\text{control}})]\} \times 100$$

Effects of ATE on the Scavenging of DPPH Radicals. The scavenging effects of extracts on DPPH radicals were estimated according to the method of Shimada et al. (*16*). In brief, 50 μL of different samples were added to 200 μL of a freshly prepared 0.1 mM DPPH solution in methanol. After thorough mixing, the solutions were kept in the dark for 50 min. Thereafter, the absorbance of the samples was measured by an Optimax automated microplate reader (Molecular Devices, San Francisco, CA) at 517 nm. The scavenger capacities were compared to a solvent control (methanol with DPPH and 20% dimethylsulfoxide (DMSO) as the blank reference). Each sample was tested in triplicate, and the values were averaged. The scavenger capacities were calculated as a percentage using the following formula:

$$\text{scavenger capacity (\%)} = [1 - (\text{absorbance}_{\text{sample-treated}} - \text{absorbance}_{\text{sample}})/\text{absorbance}_{\text{control}}] \times 100$$

Cell Culture and Stimulations. RAW 264.7 cells (murine) were obtained from Bioresource Collection and Research Center (BCRC, Food Industry Research and Development Institute, Hsinchu, Taiwan) and cultured in a 5% CO_2 atmosphere at 37 °C with Dulbecco's modified Eagle medium (DMEM) containing 10% heat-inactivated fetal bovine serum (FBS), 1% penicillin−streptomycin, and 1% glutamine. For the simulated inflammation system, cells were plated in 96-well or 10 cm dishes, allowed to grow for 18−24 h, and then treated with vehicle (0.1% DMSO), test extracts, and/or LPS, all of which were carried out under serum-free conditions.

MTT Assay for Cell Viability. RAW 264.7 macrophage cells were plated into 96-well plates at a density of 10^5 cells/well and allowed to grow for 18−24 h. Subsequently, the culture medium was replaced, and various test samples were added and treated with or without LPS (1 μg/mL) for 24 h. All test samples mentioned above were dissolved in DMSO, and the final concentration of the solvent was <0.1%. The filtered MTT solution in DMEM (serum free) was added to each well (0.5 mg of MTT/mL) and incubated at 37 °C for 2 h, and then the unreacted dye was removed. The insoluble MTT formazan crystals were dissolved in DMSO at room temperature for 15 min. At the end of this period, plates were analyzed for absorbance at 570 nm. The percentage viability of various test groups was calculated by

$$(\text{absorbance of the test group}/\text{absorbance of the control group}) \times 100$$

NO Formation. RAW 264.7 macrophage cells were treated in a manner similar to that described for examining cell viability. In brief, cells were treated with either medium alone, LPS, or test samples for 24 h. Thereafter, each supernatant (100 μL) was mixed with the same volume of Griess reagent [1% sulfanilamide in 5% phosphoric acid and 0.1% *N*-(1-naphthyl)ethylenediamine dihydrochloride in water] and allowed to react for 15 min in the dark. The formation of nitrite was reflected by the value of the absorbance at 570 nm. NO synthesis was calculated as a percentage using the following formula:

$$\text{NO synthesis (\%)} = [(\text{absorbance}_{\text{sample-treated}} - \text{absorbance}_{\text{control}})/(\text{absorbance}_{\text{LPS-treated}} - \text{absorbance}_{\text{control}})] \times 100\%$$

Western Blotting. RAW 264.7 macrophage cells were treated in a manner similar to that described for examining NO formation and cell viability. Thereafter, cells were washed twice with ice-cold PBS and then lysed in extraction lysis buffer [50 mM Tris-HCl (pH 8.0), 1 mM NaF, 150 mM NaCl, 1 mM EGTA, 1 mM phenylmethanesulfonyl fluoride, 1% NP-40, and 10 μg/mL leupeptin], followed by centrifugation at 10000*g* for 30 min at 4 °C. The cytosolic fraction (supernatant) proteins were measured using the Bradford assay, with bovine serum albumin (BSA) as a standard. Total cytosolic extracts (500 μg of protein/mL) were separated on 8% sodium dodecylsulfate (SDS)−polyacrylamide minigels for iNOS, COX-2, and β-actin detection and then transferred to an Immobilon polyvinylidene difluoride membrane (PVDF) 11 (Millipore, Bedford, MA) with transfer buffer composed of 25 mM Tris-HCl (pH 8.9), 192 mM glycine, and 20% methanol. The membrane was blocked in a 5% BSA solution for 1 h at room temperature and then incubated overnight at 4 °C with the indicated primary antibodies (at a 1:1000 dilution). After hybridization with primary antibodies, the membrane was washed with Tween 20/PBS (PBST) 3 times, incubated with an HRP-labeled secondary antibody for overnight at 4 °C, and then washed with PBST 3 more times. Final detection was performed with enhanced chemiluminescence (ECL) Western blotting reagents (Amersham Pharmacia Biotech).

Statistical Analysis. The data are presented as the mean ± standard deviation (SD). Differences between specific means were analyzed by one-way analysis of variance (ANOVA) using the SPSS system, version 11.0 (SPSS, Chicago, IL). Group means were compared using one-way ANOVA and Duncan's multiple-range test. For a comparison between two groups, Student's *t* test was used. The difference between

Table 1. Antioxidative and Anti-inflammatory Effects of Various Fractions and Subfractions of the Ethanolic Extract of Adlay Testa (ATE)

	antioxidation[a]			anti-inflammation[b]	
	LDL CD	TBARS			
	δT_{lag} (h)[c]	inhibition (%)	DPPH scavenger capacity (%)	NO synthesis (%)	cell viability (%)
Trolox	7.99 ± 0.01	44.6 ± 2.8	71.3 ± 2.39	77.2 ± 0.9	120 ± 4
			extract/fraction		
ATE-Hex	0.74 ± 0.00	−18.2 ± 1.3	13.3 ± 2.88	56.7 ± 1.0	126 ± 4
ATE-Ea	>12	89.2 ± 0.8	26.7 ± 2.01	53.0 ± 0.4	134 ± 3
ATE-Bu	>12	91.5 ± 0.1	34.2 ± 2.73	76.1 ± 1.4	112 ± 9
ATE-H_2O	1.52 ± 0.62	−41.9 ± 1.4	12.2 ± 1.98	101 ± 1.3	117 ± 8
			ATE-Ea subfraction		
a	−0.15 ± 0.01	−35.5 ± 3.4	13.6 ± 2.87	31.1 ± 0.9	99 ± 17
b	−0.02 ± 0.00	−32.7 ± 0.8	12.4 ± 1.45	9.6 ± 0.8	84 ± 6
c	2.42 ± 0.07	−37.4 ± 1.3	10.2 ± 0.94	4.1 ± 0.8	106 ± 7
d	5.69 ± 0.26	−38.3 ± 1.9	17.6 ± 1.96	1.9 ± 0.8	117 ± 7
e	>12	54.8 ± 0.1	18.4 ± 1.95	0.9 ± 0.8	113 ± 7
f	>12	86.7 ± 0.1	21.0 ± 1.18	15.7 ± 0.8	148 ± 4
g	2.19 ± 0.04	−55.5 ± 1.3	13.7 ± 1.75	27.3 ± 0.8	111 ± 12
h	5.28 ± 0.08	76.9 ± 2.5	22.2 ± 3.96	37.0 ± 0.9	93.6 ± 19
			ATE-Bu subfraction		
A	0.48 ± 0.26	−42.4 ± 13.9	13.8 ± 1.66	88.9 ± 4.0	95 ± 4
B	−0.12 ± 0.14	−34.3 ± 4.5	10.0 ± 1.67	74.3 ± 5.0	95 ± 2
C	>12	86.2 ± 2.1	24.1 ± 1.65	66.8 ± 8.7	96 ± 4
D	>12	80.0 ± 7.2	29.5 ± 2.27	78.2 ± 6.7	97 ± 5
E	8.05 ± 1.03	76.7 ± 2.1	20.1 ± 0.21	92.6 ± 1.0	94 ± 1
F	>12 h	79.5 ± 2.8	19.9 ± 2.52	83.8 ± 7.9	97 ± 3

[a] Concentrations of Trolox, the extract/fraction group, and subfraction groups used in the antioxidant were 10, 25, and 10 μg/mL, respectively. [b] Concentrations of all groups used in anti-inflammation were 25 μg/mL. [c] Values are expressed as hours from the difference in the lag phase between various sample-treated groups and the $CuSO_4$-treated group.

two means was considered statistically significant when $p < 0.05$ and highly significant when $p < 0.01$.

RESULTS

3.1. Antioxidant Effects of Various Fractions and Subfractions of ATE. We investigated the antioxidative activities of various fractions of ATE with the LDL oxidation assay and made comparisons to the DPPH radical-scavenging capacity. **Table 1** summarizes the retardation effect of LDL diene conjugation and the inhibitory effect of TBARS, respectively. ATE-Ea and ATE-Bu (25 μg/mL) both had greater antioxidative effects than ATE-Hex and ATE-H_2O in retardation of Cu^{2+}-induced diene conjugation (>12 h) and inhibition of the formation of TBARS (89 and 92%, respectively). In comparison to the protective effects on LDL oxidation, both the ATE-Ea and ATE-Bu (25 μg/mL) demonstrated the greatest free-radical scavenging abilities (27 and 34%, respectively). Thereafter, we used a regression analysis to correlate the results of TBARS formation and DPPH-scavenging activity, and the result displayed a high correlation coefficient between them (data not shown, $R^2 = 0.99$).

For the antioxidative effects described above (**Table 1**), both ATE-Ea and ATE-Bu displayed greater antioxidative activities than ATE-Hex and ATE-H_2O. Thus, ATE-Ea was separated into eight subfractions (a−h) and ATE-Bu was divided into six subfractions (A−F) accordingly by chromatography for further examination. The antioxidative activity of the ATE-Ea subfractions (a−h) in the LDL oxidation assay and DPPH radical-scavenging capacity are shown in **Table 1**. Subfractions e and f (10 μg/mL) demonstrated effects of retarding Cu^{2+}-induced diene conjugation (>12 h) and inhibiting the formation of TBARS (55 and 87%, respectively) with greater efficacy than the others. Subfraction f (10 μg/mL) expressed higher DPPH radical-scavenging activity (21%) than the other subfractions of ATE-Ea. Subsequently, we used a regression analysis to correlate the results of TBARS formation with the DPPH-scavenging activity, which yielded a high correlation coefficient (data not shown, $R^2 = 0.75$).

The antioxidative and antiradical activities of ATE-Bu subfractions (A−F) on the LDL oxidation assay and DPPH radical-scavenging capacity are shown in **Table 1**. Subfractions C, D, and F (10 μg/mL) demonstrated effects of retardation of Cu^{2+}-induced diene conjugation (>12 h) and inhibition of the formation of TBARS (by 86, 80, and 80%, respectively) with greater efficacy than the others. Subfraction D provided the highest values of DPPH radical-scavenging activity (30%) of all of the subfractions of ATE-Bu.

3.2. Effects of Various Fractions of ATE on LPS-Induced Cell Survival and NO Formation in RAW 264.7 Cells. The cell viability and NO formation of RAW 264.7 macrophages cells were tested after treatment with different fractions of ATE (25 μg/mL) and LPS (1 μg/mL) for 24 h. **Table 1** indicates that the survivability of macrophages was not affected by the different ATE fractions and the synthesis of NO was lowered by ATE-Hex, ATE-Ea, and ATE-Bu (by 57, 53, and 76%, respectively).

Table 1 indicates that the viability of macrophages was not affected by the addition of LPS (1 μg/mL) or different subfractions (25 μg/mL) of ATE-Ea or ATE-Bu for 24 h, except for the ATE-Ea-b subfraction (84%). The results showed that the synthesis of NO was lowered by various ATE-Ea subfractions in the order of e (0.9%) < d (1.9%) < c (4.1%) < b (9.6) < g (27%) < a (31%) < h (37%). NO synthesis was still suppressed by ATE-Bu subfractions with the suppression in the order of C (67%) < B (74%) < D (78%) < F (84%) < A (89%) < E (93%); however, the inhibitory effects of the ATE-Ea subfractions were better than those of ATE-Bu (**Table 1**).

3.3. Effects of ATE-Ea, ATE-Bu, ATE-Ea-e, and ATE-Bu-C on LPS-Induced COX-2 and iNOS Protein Expressions in RAW 264.7 Cells. COX-2 and iNOS are both critical and necessary components of the inflammatory pathway, leading to the formation of NO and PGE_2 in murine macrophages (*17*).

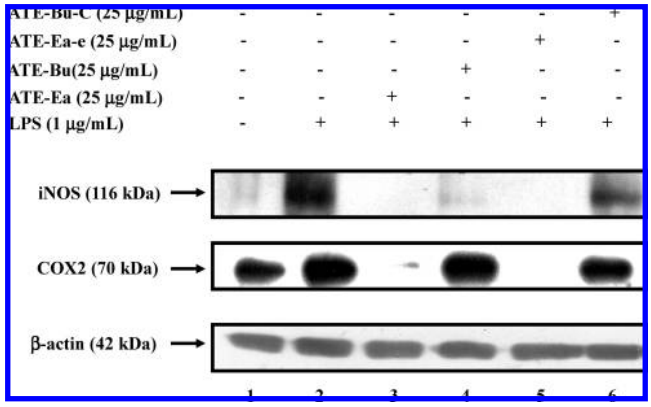

Figure 2. Effects of ATE-Ea, ATE-Bu, ATE-Ea-e, and ATE-Bu-C on LPS-induced iNOS and COX-2 protein expressions in RAW 264.7 cells. Cells were treated with (lane 2) or without (lane 1) 1 μg/mL LPS, and the fractions ATE-Ea (lane 3) and ATE-Bu (lane 4) or subfractions ATE-Ea-e (lane 5) and ATE-Bu-C (lane 6) were co-incubated with LPS-treated cells for 20 h. At the end of incubation, equal amounts of total proteins (500 μg/mL) were subjected to SDS−PAGE and the expressions of iNOS, COX-2, and β-actin protein were detected by Western blotting using specific antibodies.

Thus, Western blotting was used to determine whether any inhibitory effects on the protein expressions of COX-2 and iNOS were evident after the application of various test samples. As shown in **Figure 2**, in contrast, murine macrophage cells treated with LPS alone showed dramatic inductions of COX-2 and iNOS. Treatment with ATE-Ea (lane 3), ATE-Bu (lane 4), ATE-Ea-e (lane 5), and ATE-Bu-C (lane 6) inhibited LPS-induced COX-2 and iNOS protein expressions. The data indicated that 25 μg/mL of ATE-Ea and ATE-Ea-e had greater inhibitory capacities toward iNOS and COX-2 protein expressions than ATE-Bu and ATE-Bu-C.

3.4. Analysis of the Phenolic Compounds in ATE-Ea and ATE-Bu by HPLC. Analytical plots of phenolic compounds in ATE-Ea and ATE-Bu are shown in **Figure 3**. There were 16 compounds contained in the standard curve (**Figure 3A**): (**2**) CGA, (**3**) VA, (**4**) CA, (**6**) 4HA, (**8**) syringaldehyde, (**11**) 6-methoxy-3*H*-benzoxazol, and (**16**) GMBO were purified in this study. (**1**) Gallic acid (GA), (**5**) syringic acid (SA), (**7**) *p*-coumaric acid (PCA), (**9**) ferulic acid (FA), (**12**) quercetin, and **(13)** narigenin were found in the adlay hull (*5*). Compounds **10** (sinapaldehyde), **14** (apigenin), and **15** (5-hydroxy-7-methoxy-4′-acetyl-isoflavone) were obtained in the adlay seed, and none has yet been published. In comparison to the retention times of the standard curve (**Figure 3A**), the separation of phenolic compounds in ATE-Ea is presented in **Figure 3B**. Peaks corresponded to (**1**) GA, (**2**) CGA, (**3**) VA, (**4**) CA, (**5**) SA, (**6**) 4HA, (**7**) PCA, and (**9**) FA. Subsequently, ATE-Ea-e, the bioguided subfraction of ATE-Ea was further analyzed by HPLC. The three peaks corresponded to VA, PCA, and FA (**Figure 3C**).

Figure 3D shows the HPLC chromatogram of ATE-Bu, on which were three marked peaks in the analytical. Subsequently, ATE-Bu-C, the bioguided subfraction of ATE-Bu, was further analyzed by HPLC. The three peaks corresponded to CGA, CA, and GMBO (**Figure 3E**).

3.5. Effects of Phenolic Compounds in ATE on Antioxidation and LPS-Induced NO Formation in RAW 264.7 Cells. The following components were found in ATE after purification and HPLC analysis: GA, CGA, VA, CA, SA, GMBO, 4HA, PCA, and FA. The antioxidative, antiradical, and anti-inflammatory activities of various phenolic compounds of

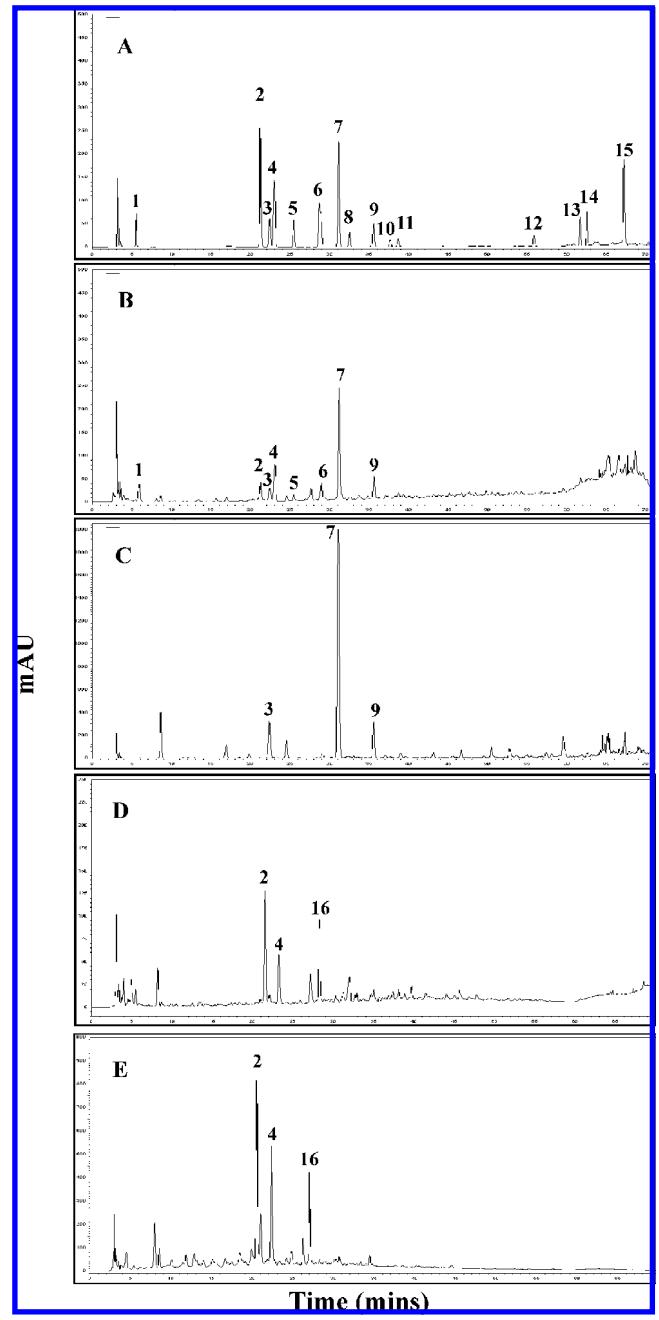

Figure 3. HPLC chromatogram of (A) phenolic compound standards isolated from AT, (B) ATE-Ea fraction, (C) ATE-Ea-e subfraction, (D) ATE-Bu fraction, and (E) ATE-Bu-C subfraction separated from AT. **1**, GA; **2**, CGA; **3**, VA; **4**, CA; **5**, SA; **6**, 4HA; **7**, PCA; **8**, syringaldehyde; **9**, FA; **10**, sinapaldehyde; **11**, 6-methoxy-3*H*-benzoxazol; **12**, quercetin; **13**, narigenin; **14**, apigenin; **15**, 5-hydroxy-7-methoxy-4′-acetyl-isoflavone; **16**, GMBO.

ATE in the LDL oxidation assay, DPPH radical-scavenging capacity, and LPS-induced NO formation in RAW 264.7 cells are shown in **Table 2**. GA, CGA, CA, and FA (10 μg/mL) had the greatest effects on retarding Cu^{2+}-induced diene conjugation (>12 h), and the inhibitory effect on TBARS decreased in the order of CA (100%) > GA (97.7%) > FA (96.8%) > CGA (93.3%) > PCA (56.6%) > VA (31.0%) > 4HA (24.4%) > GMBO (3.19%) > SA (−47.8%). EC_{50} values of the DPPH radical-scavenging capacity of various phenolic compounds were in the increasing order of GA (0.19 μg/mL) > FA (1.40 μg/mL) > SA (3.26 μg/mL) > CA (6.26 μg/mL) > CGA (6.99 μg/mL), and the EC_{50} values of VA, GMBO, 4HA, and PCA all exceeded 20 μg/mL.

Table 2. Cu^{2+}-Induced LDL Oxidative, DPPH Radical-Scavenger Capacity, LPS-Induced NO Formation Effects on RAW 264.7 Cells of Various Components Isolated from ATE-Ea and ATE-Bu and the Contents in Various Subfractions

	LDL oxidation					
	LDL CD	TBARS	DPPH scavenger	NO inhibition		contents
	δT_{lag} (h)[a]	inhibition (%)	capacity (EC_{50}, μg/mL)	(EC_{50}, μg/mL)	Rt[b] (min)	(mg/g subfraction)[c]
resveratrol[d]	>12	90.4 ± 0.4	14.1 ± 0.83	4.9 ± 0.4		
gallic acid[e]	>12	97.7 ± 1.4	0.19 ± 0.00	7.1 ± 1.5	5.5	
chlorogenic acid	>12	93.3 ± 2.8	6.99 ± 0.31	16.6 ± 0.8	21.2	30.3 ± 4.7
vanillic acid	1.70 ± 0.11	31.0 ± 6.7	>20	517 ± 12	22.3	1.31 ± 0.08
caffeic acid	>12	100 ± 3.1	6.26 ± 0.92	15.9 ± 4.8	23.0	9.02 ± 1.22
syringic acid	−0.55 ± 0.05	−47.8 ± 3.0	3.26 ± 0.06	1.7 ± 0.3	25.4	
2-*O*-β-glucopyranosyl-7-methoxy-4(^2H)-benzoxazin-3-one	−2.34 ± 0.05	3.19 ± 1.2	>20	ND	27.8	189 ± 16
4-hydroxyacetophenone	0.16 ± 0.01	24.4 ± 6.0	>20	25.3 ± 2.5	28.9	
p-coumaric acid	−0.57 ± 0.05	56.6 ± 1.7	>20	437 ± 23	31.1	3.89 ± 0.12
ferulic acid	>12	96.8 ± 0.6	1.40 ± 0.13	16.3 ± 5.7	35.6	0.05 ± 0.00

[a] Values are expressed as hours from the difference in the lag phase between various treated groups and the $CuSO_4$-treated group. The concentration of various phenolic components used in this system, except for the GA group, was 10 μg/mL. [b] Retention times corresponding to standards. [c] Values were calculated as the contents per gram of the subfractions. [d] Resveratrol was used as the positive control. [e] GA at 2.5 μg/mL was used in this system because of its discoloration character at higher concentrations.

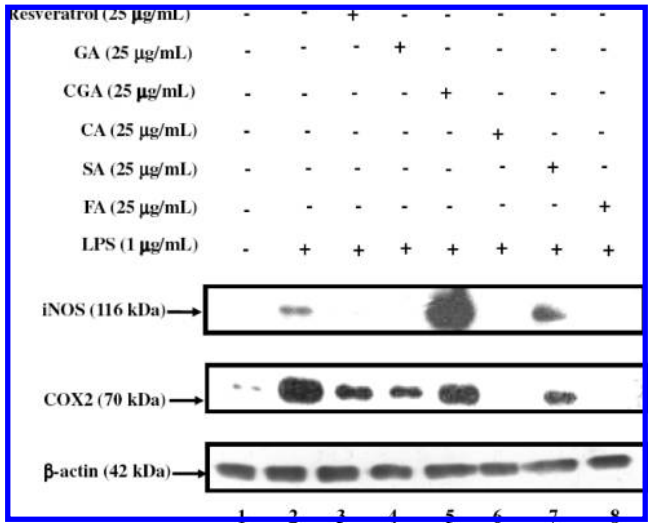

Figure 4. Effects of the active components isolated from ATE on LPS-induced iNOS and COX-2 protein expressions in RAW 264.7 cells. Cells were treated with (lane 2) or without (lane 1) 1 μg/mL LPS, and the components isolated from ATE were co-incubated with LPS-treated cells for 20 h (lanes 3−8). At the end of incubation, equal amounts of total proteins (500 μg/mL) were subjected to SDS−PAGE and the expressions of iNOS, COX-2, and β-actin protein were detected by Western blotting using specific antibodies. Lane 3, resveratrol (positive control); lane 4, GA; lane 5, CGA; lane 6, CA; lane 7, SA; lane 8, FA.

In the LPS/RAW 264.7 macrophage cell system, EC_{50} values for inhibiting NO formation were in the increasing order of SA (1.7 μg/mL) < GA (7.1 μg/mL) < CA (15.9 μg/mL) < FA (16.3 μg/mL) < CGA (16.6 μg/mL) < 4HA (25.3 μg/mL) < PCA (437 μg/mL) < VA (517 μg/mL) < GMBO (not detected).

3.6. Effects of Resveratrol, GA, CGA, CA, SA, and FA on LPS-Induced COX-2 and iNOS Protein Expressions in RAW 264.7 Cells. As shown in **Figure 4**, in contrast, murine macrophage cells treated with LPS alone showed dramatic inductions of COX-2 and iNOS (lane 2). Cells treated with resveratrol, GA, CA, and FA (lanes 3, 4, 6, and 8, respectively) inhibited LPS-induced COX-2 and iNOS protein expressions, and the expression of iNOS protein by LPS-induced RAW 264.7 cells markedly improved in the CGA-treated group (lane 5). The data indicated that the inhibitory actions on iNOS and COX-2 protein expressions by GA, CA, and FA may be partially responsible for the inhibition of NO formation by ATE.

DISCUSSION

In the present study, ATE expressed antioxidative and antiradical effects through LDL protection and DPPH radical-scavenging capacity and the inflammatory reaction was inhibited by ATE via downregulating the expressions of iNOS and COX-2 protein.

Several lines of evidence indicate that oxidative stress and inflammation play important roles in atherosclerosis. An increase in the LDL content causes the early phase of atherosclerosis according to the oxidative modification hypothesis; oxidation of LDL is the most likely cause of atherogenesis (*3*). As described by Abuja et al. (*18*), recruited antioxidants may, where appropriate, prolong the lag phase in Cu^{2+}-mediated LDL oxidation for a considerable time after the consumption of tocopherol. The consumption of food rich in natural antioxidants has been related to prevention of atherosclerosis. Berliner et al. (*1*) noted that the initial processes of atherosclerosis were directly related to the oxidation of lipids in LDLs, and these oxidized (ox)-LDLs subsequently activate inflammatory events. Thus, the effects of various samples on the inhibition of Cu^{2+}-mediated LDL oxidation and LPS-induced inflammation in RAW 264.7 macrophages were investigated in the study.

Resveratrol is a naturally occurring compound, which was first observed during infection of detached grapevine leaves in 1976 by Langcake and Pryce (*19*), and has been shown to modulate the risk of atherogenesis via inhibition of LDL oxidation (*2*). In addition, the effects of magnesium tanshinoate B (MTB), purified from Danshen, on the inhibition of LDL oxidation were also well-characterized (*20*). Hyperlipidemic smokers supplied with adlay and young barley leaf extract showed decreased concentrations of plasma lipids coupled with an increasing lag phase in LDL oxidation (*21*). In this study, subfractions ATE-Ea, ATE-Bu, ATE-Ea-e, and ATE-Bu-C yielded the best performance with respect to retardation of LDL oxidation (**Table 1**). The increased formation of ROS contributes to atherosclerosis and causes activation of neutrophils, lipid oxidation, protein modification, and DNA breakage (*22*). According to **Table 1**, at least in part, we presumed that the combined effects of the processes described above can protect LDL against oxidation, possibly by a lowering oxidative stress.

It has been well-established that there is a large amount of NO formation induced by LPS and cytokines, suggesting a high correlation with various pathophysiological processes, including inflammation, carcinogenesis, and atherosclerosis (*23*). In light of this, the LPS-induced NO formation by RAW 264.7 cells was used to study the inhibitory effects evident in the initial stages of inflammation. Subfractions ATE-Ea, ATE-Ea-e, ATE-Bu, and ATE-Bu-C showed the best performances of all fractions and subfractions (**Table 1**). Subsequently, ATE-Ea, ATE-Ea-e, ATE-Bu, and ATE-Bu-C were chosen to investigate the expressions of inflammation-related proteins because of their effects on the inhibition of LDL oxidation and NO formation. Inano and Onoda (*24*) postulated that NO is synthesized by NOS in various animal cells and tissues. The expression of NOS in macrophages is in the form of iNOS and is activated by either LPS or various cytokines (*23*). Thus, **Figure 2** shows that ATE-Ea, ATE-Bu, ATE-Ea-e, and ATE-Bu-C inhibited the expression of iNOS. This indicates that ATE-Ea, ATE-Bu, ATE-Ea-e, and ATE-Bu-C possibly inhibited the formation of NO through the expression of iNOS protein. Extracts of *Gynostemma pentaphyllum* were also shown to inhibit LPS-induced NO production by blocking iNOS expression (*25*). The effect of various anti-inflammatory drug actions occurs at least via the inhibition of prostaglandin (PG) synthesis, which is mediated by COX (*26*). COX exists in two isoforms, COX-1 and COX-2, each with distinct expression patterns in various cell types. COX-1 has been suggested to function by maintaining physiological levels of PGs in the gastrointestinal (GI) tract. Unlike COX-1, COX-2 is subjected to rapid induction by inflammatory cytokines and LPS (*27*). In a rabbit model of atherosclerosis, it was shown that the expression of COX-2 induced the dysfunction of endothelial cells (*3*). Wang et al. noted that the inhibition of iNOS and COX-2 protein expression retarded inflammatory reactions and protected against cardiovascular disease (*28*). As shown in **Figure 2**, COX-2 protein expression was markedly inhibited by ATE-Ea and ATE-Ea-e. This indicates that ATE-Ea may be a COX-2 inhibitor and the major active subfraction was ATE-Ea-e.

It was reported that phenolic phytochemicals show strong antioxidative and anti-inflammatory activities (*29*). In the present study, the following components were found in ATE after purification and HPLC analysis: GA, CGA, VA, CA, SA, GMBO, 4HA, PCA, and FA. The major compounds of ATE-Ea-e were VA, PCA and FA, and the major compounds of ATE-Bu-C were CGA, CA, and GMBO (**Figure 3**). GA, CGA, CA, SA, and FA showed the greatest antioxidant and anti-inflammatory effects through downregulating the expression of iNOS or COX-2 protein (**Table 2** and **Figure 4**). These results also suggest that the antioxidative and anti-inflammatory activities of ATE-Ea and ATE-Bu are related to their phenolic compounds. However, the expression of iNOS protein by LPS-induced RAW 264.7 cells was markedly increased in the CGA-treated group; thus, the modulatory effect of ATE-Bu on the expression of iNOS protein was better than that of ATE-Bu-C possibly because of an increased CGA content. On the other hand, although GMBO is a major component of ATE-Bu and ATE-Bu-C (parts **D** and **E** of **Figure 3**), it expressed weak activity in the Cu^{2+}/LDL system, as an antiradical of DPPH (EC_{50} > 20 μg/mL), and LPS-induced NO formation in RAW 264.7 cells (EC_{50} was not detected until 1 mg/mL, **Table 2**) in this study. However, Otsuka et al. pointed out that the aglycone of GMBO displays strong anti-inflammatory activity. *In vivo*, the glycoside is hydrolyzed; thus, different results might be expected (*30*).

In conclusion, ATE inhibited both iNOS and COX-2 protein expressions and reduced LDL oxidation. These results indicate that the ATE has antioxidative and anti-inflammatory effects, which are the most important attributes in preventing atherosclerosis, and the efficient functional fractions ATE-Ea-e and ATE-Bu-C were separated by column chromatography. Further investigations of the treatment of atherosclerosis *in vivo* with ATE may be helpful for patients with different cardiovascular lesions.

ABBREVIATIONS USED

AT, adlay testa; ATE, adlay testa ethanolic extract; AOM, azoxymethane; BCRC, Bioresource Collection and Research Center; BSA, bovine serum albumin; AHM-Bu, butanolic fraction of the methanolic extract of adlay hull; CA, caffeic acid; CGA, chlorogenic acid; CD, conjugated diene; COX-2, cyclooxygenase 2; DPPH, 2,2′-diphenyl-1-picrylhydrazyl; ATE-Ea, ethyl acetate fraction of the adlay testa ethanolic extract; FA, ferulic acid; FBS, fetal bovine serum; GA, gallic acid; GI, gastrointestinal; HPLC, high-performance liquid chromatography; 4HA, 4-hydroxyacetophenone; Trolox, 6-hydroxy-2,5,7,8-tetramethylchroman-2-carboxylic acid; iNOS, inducible nitric oxide synthase; LPS, lipopolysaccharide; LDL, low-density lipoprotein; MTB, magnesium tanshinoate B; ASM, methanolic extract of adlay seed; NNK, 4-(methylnitrosamino)-1-(3-pyridyl)-1-butanone; ATE-Bu, *n*-butanol fraction of the adlay testa ethanolic extract; ATE-Hex, *n*-hexane fraction of the adlay testa ethanolic extract; NO, nitric oxide; GMBO, 2-*O*-β-glucopyranosyl-7-methoxy-4(^2H)-benzoxazin-3-one; PCA, *p*-coumaric acid; PGE, prostaglandin E; ROS, reactive oxidative species; SA, syringic acid; TBA, 2-thiobarbituric acid; TBARS, thiobarbituric-acid-reactive substances; TCA, trichloroacetic acid; VA, vanillic acid; ATE-H_2O, water fraction of the adlay testa ethanolic extract.

LITERATURE CITED

(1) Berliner, J. A.; Navab, M.; Fogelman, A. M.; Frank, J. S.; Demer, L. L.; Edwards, P. A.; Watson, A. D.; Lusis, A. J. Atherosclerosis: Basic mechanisms. Oxidation, inflammation, and genetics. *Circulation* **1995**, *91*, 2488–2496.

(2) Frémont, L.; Belguendouz, L.; Delpal, S. Antioxidant activity of resveratrol and alcohol-free wine polyphenols related to LDL oxidation and polyunsaturated fatty acids. *Life Sci.* **1999**, *64*, 2511–2521.

(3) Hernández-Presa, M. A.; Martin-Ventura, J. L.; Ortego, M.; Gomez-Hernandez, A.; Tunon, J.; Hernandez-Vargas, P. Atorvastatin reduces the expression of cyclooxygenase-2 in a rabbit model of atherosclerosis and in cultured vascular smooth muscle cells. *Atherosclerosis* **2002**, *160*, 49–58.

(4) Sen, R.; Baltimore, D. Multiple nuclear factors interact with the immunoglobulin enhancer sequences. *Cell* **1986**, *46*, 705–716.

(5) Hsia, S. M.; Chiang, W.; Kuo, Y. H.; Wang, P. S. Downregulation of progesterone biosynthesis in rat granulosa cells by adlay (*Coix lachryma-jobi* L. var. *ma-yuen* Stapf) bran extracts. *Int. J. Impotence Res.* **2006**, *18*, 264–274.

(6) McKevith, B. Nutritional aspects of cereals. *Nutr. Bull.* **2004**, *29*, 111–142.

(7) Kuo, C. C.; Chiang, W.; Liu, G. P.; Chien, Y. L.; Chang, J. Y.; Lee, C. K.; Lo, J. M.; Huang, S. L.; Shih, M. C.; Kuo, Y. H. 2,2′-Diphenyl-1-picrylhydrazyl radical-scavenging active components from adlay (*Coix lachryma-jobi* L. var. *ma-yuen* Stapf) hulls. *J. Agric. Food Chem.* **2002**, *50*, 5850–5855.

(8) Seo, W. G.; Pae, H. O.; Chai, K. Y.; Yun, Y. G.; Kwon, T. H.; Chung, H. T. Inhibition effects of methanol extract of seeds of Job's tears (*Coix lachryma-jobi* L. var. *ma-yuen*) on nitric oxide

and superoxide production in RAW 264.7 macrophages. *Immunopharmacol. Immunotoxicol.* **2000**, *22*, 545–554.
(9) Hsia, S. M.; Yeh, C. L.; Kuo, Y. H.; Wang, P. S.; Chiang, W. Effects of adlay (*Coix lachryma-jobi* L. var. *ma-yuen* Stapf) hull extracts on the secretion of progesterone and estradiol *in vivo* and *in vitro*. *Exp. Biol. Med.* **2007**, *232*, 1181–1194.
(10) Chang, H. C.; Huang, Y. C.; Hung, W. C. Antiproliferative and chemopreventive effects of adlay seed on lung cancer in vitro and in vivo. *J. Agric. Food Chem.* **2003**, *51*, 3656–3660.
(11) Shih, C. K.; Chiang, W.; Kuo, M. L. Effects of adlay on azoxymethane-induced colon carcinogenesis in rats. *Food Chem. Toxicol.* **2004**, *42*, 1339–1347.
(12) Lee, M. Y.; Lin, H. Y.; Cheng, F.; Chiang, W.; Kuo, Y. H. Isolation and characterization of new lactam compounds that inhibit lung and colon cancer cells from adlay (*Coix lachryma-jobi* L. var. *ma-yuen* Stapf) bran. *Food Chem. Toxicol.* **2008**, *46*, 1933–1939.
(13) Yen, G. C.; Duh, P. D.; Huang, D. W.; Hsu, C. L.; Fu, T. Y. C. Protective effect of pine (*Pinus morrisonicola* Hay.) needle on LDL oxidation and its anti-inflammatory action by modulation of iNOS and COX-2 expression in LPS-stimulated RAW 264.7 macrophages. *Food Chem. Toxicol.* **2008**, *46*, 175–185.
(14) Bourne, L.; Rice-Evans, C. A. The effect of the phenolic antioxidant ferulic acid on the oxidation of low density lipoprotein depends on the pro-oxidant used. *Free Radical Res.* **1997**, *27*, 337–344.
(15) Yagi, K. A simple fluorometric assay for lipids peroxides in blood serum or plasma. *CRC Handbook of Free Radicals and Antioxidants in Biomedicine*; CRC Press: Boca Raton, FL, 1989; Vol. 3, p 215.
(16) Shimada, K.; Fujikawa, K.; Yahara, K.; Nakamura, T. Antioxidative properties of xanthan on the autoxidation of soybean oil in cyclodextrin emulsion. *J. Agric. Food Chem.* **1992**, *40*, 945–948.
(17) Shin, S. D.; Fabris, M.; Ferrari, V.; Carbonare, M. D.; Leon, A. Quercetin protects cutaneous tissue-associated cell types including sensory neurons from oxidative stress induced by glutathione depletion: Cooperative effects of ascorbic acid. *Free Radical Biol. Med.* **2004**, *22*, 669–678.
(18) Abuja, P. M.; Albertini, R.; Esterbauer, H. Simulation of the induction of oxidation of low-density lipoprotein by high copper concentrations: Evidence for a nonconstant rate of initiation. *Chem. Res. Toxicol.* **1997**, *10*, 644–651.
(19) Langcake, P.; Pryce, R. J. The production of resveratrol by *Vitis vinifera* and other members of the Vitaceae as a response to infection or injury. *Physiol. Mol. Plant Pathol.* **1976**, *9*, 77–86.
(20) Karmin, O.; Edward, G. L.; Rema, V.; Kathy, K. W.; Au-Yeung, D. Y. Z.; Yaw, L. S. Magnesium tanshinoate B (MTB) inhibits low density lipoprotein oxidation. *Life Sci.* **2001**, *68*, 903–912.
(21) Yu, Y. M.; Chang, W. C.; Liu, C. S.; Tsai, C. M. Effect of young barley leaf extract and adlay on plasma lipids and LDL oxidation in hyperlipidemic smokers. *Biol. Pharm. Bull.* **2004**, *27*, 802–805.
(22) Singh, U.; Devaraj, S.; Jialal, I. Vitamin E, oxidative stress, and inflammation. *Annu. Rev. Nutr.* **2005**, *25*, 151–174.
(23) Chen, Y. C.; Shen, S. C.; Lee, W. R.; Hou, W. C.; Yang, L. L.; Lee, T. J. F. Inhibition of nitric oxide synthase inhibitors and lipopolysaccharide included inducible NOS and cyclooxygenase-2 gene expression by rutin, quercetin, and quercetin pentaacetate in RAW 264.7 macrophages. *J. Cell. Biochem.* **2001**, *82*, 537–548.
(24) Inano, H.; Onoda, M. Role of nitric oxide in radiation induced initiation of mammary tumorigenesis in rats. *Nitric Oxide* **2003**, *8*, 144–148.
(25) Aktan, F.; Henness, S.; Roufogalis, B. D.; Ammit, A. J. Gypenosides derived from *Gynostemma pentaphyllum* suppress NO synthesis in murine macrophages by inhibiting iNOS enzymatic activity and attenuating NF-κB-mediated iNOS protein expression. *Nitric Oxide* **2003**, *8*, 235–242.
(26) Vane, J. R.; Bakhle, Y. S.; Botting, R. M. Cyclooxygenases 1 and 2. *Annu. Rev. Pharmacol.* **1998**, *38*, 97–120.
(27) Grosser, T.; Fries, S.; FitzGerald, G. A. Biological basis for the cardiovascular consequences of COX-2 inhibition: Therapeutic challenges and opportunities. *J. Clin. Invest.* **2006**, *116*, 4–14.
(28) Wang, B. S.; Chen, J. H.; Liang, Y. C.; Duh, P. D. Effects of Welsh onion on oxidation of low-density lipoprotein and nitric oxide production in macrophage cell line RAW 264.7. *Food Chem.* **2005**, *91*, 147–155.
(29) Kris-Etherton, P. M.; Lefevre, M.; Beecher, G. R.; Gross, M. D.; Keen, C. L.; Etherton, T. D. Bioactive compounds in nutrition and health—Research methodologies for establishing biological function: The antioxidant and anti-inflammatory effects of flavonoids on atherosclerosis. *Annu. Rev. Nutr.* **2004**, *24*, 511–538.
(30) Otsuka, H.; Hirai, Y.; Nagao, T.; Yamasaki, K. Anti-inflammatory activity of benzoxazinoids from roots of *Coix lachryma-jobi* L. var. *ma-yuen*. *J. Nat. Prod.* **1988**, *51*, 74–79.

Received for review October 20, 2008. Revised manuscript received December 19, 2008. Accepted January 31, 2009.

JF803255P